Front. Chem. Sci. Eng. 2024, 18(4): 41
https://doi.org/10.1007/s11705-024-2402-8

RESEARCH ARTICLE

Autohydrolysis treatment of bamboo and potassium oxalate ($K_2C_2O_4$) activation of bamboo product for CO_2 capture utilization

Dang Duc Viet[1,2], **Doan Thi Thao**[1,2], **Khuong Duy Anh**[1], **Toshiki Tsubota** (✉)[1,3]

1 Department of Materials Science, Faculty of Engineering, Kyushu Institute of Technology, Fukuoka 804-8550, Japan
2 Vietnamese Academy of Forest Sciences, Hanoi 10000, Vietnam
3 Collaborative Research Centre for Green Materials on Environmental Technology, Kyushu Institute of Technology, Fukuoka 808-0196, Japan

Abstract Typically, the hydroxide agents, such as sodium hydroxide and potassium hydroxide, which have corrosive properties, are used in the carbon activation process. In this study, potassium oxalate ($K_2C_2O_4$), a less toxic and non-corrosive activating reagent, was used to synthesize activated carbon from the solid residue after autohydrolysis treatment. The effect of the autohydrolysis treatment and the ratio of the $K_2C_2O_4$/solid residue are presented in this study. Moreover, the comparison between the activated carbon from bamboo and biochar from the solid residue are also reported. The resulting activated carbon from the solid residue exhibited a high surface area of up to 1432 $m^2 \cdot g^{-1}$ and a total pore volume of up to 0.88 $cm^3 \cdot g^{-1}$. The autohydrolysis treatment enhanced the microporosity properties compared to those without pretreatment of the activated carbon. The microporosity of the activated carbon from the solid residue was dominated by the pore width at 0.7 nm, which is excellent for CO_2 storage. At 25 °C and 1.013 × 10^5 Pa, the CO_2 captured reached up to 4.1 $mmol \cdot g^{-1}$. On the other hand, the ratio between $K_2C_2O_4$ and the solid residue has not played a critical role in determining the porosity properties. The ratio of the $K_2C_2O_4$/solid residue of 2 could help the carbon material reach a highly microporous textural property that produces a high carbon capture capacity. Our finding proved the benefit of using the solid residue from the autohydrolysis treatment as a precursor material and offering a more friendly and sustainable activation carbon process.

Keywords activated carbon, bamboo, biochar, CO_2 capture, potassium oxalate

Received October 10, 2023; accepted December 19, 2023;
online January 29, 2024

E-mail: tsubota@che.kyutech.ac.jp

1 Introduction

Currently, climate change and global warming have been significant threats worldwide. Their main causes are greenhouse gas and carbon dioxide emissions from burning fossil fuels [1]. Many efforts have been developed to reduce carbon dioxide emissions, focusing on CO_2 capture and adsorption [2,3]. Although the amine solution is considered as a mature method for CO_2 capture, it has a significant energy penalty and instrument corrosive [4]. Thus, biochar, with an effective cost and high-efficiency capture capacity, is a promising material for carbon dioxide storage [5,6].

Biochar is a material produced from biomaterials, such as wood and bamboo, and is pyrolyzed at high temperatures with low or no oxygen [7]. The advantages of biochar that make it occupy an important position in CO_2 capture are that it can be made from many kinds of waste materials [8,9]. Thus, this material is more environmentally sustainable and cost-effective than a metal-organic frame [10,11]. Among the prospective biochars, bamboo is an abundant renewable resource with more than 1600 species and 36 million hectares worldwide [10,12]. Bamboo is well known as one of the fastest-growing trees and has had many applications in our lives for thousands of years, including biochar, handicrafts, furniture, and construction material [13−15]. The market value for bamboo products was more than 3.7 billion US dollars as of 2019 [16].

The bamboo shoot is known as a healthy food with plenty of acid amines and vitamins necessary for our bodies [17]. Furthermore, extractive components from bamboo culms and leaves, including sugar (i.e., polysaccharides, xylooligosaccharides), are attractive resources for food additives and pharmaceuticals,

including antioxidant and cancer treatments [18,19]. Sugar from biomass, such as bamboo, can be extracted by physical pretreatments such as autohydrolysis, hydrothermal, and chemical pretreatment methods, including alkaline extraction and acid extraction [20−22]. It has been stated that the pre-treatment process is necessary and is a promising method for increasing the extraction yield [20]. In addition, the proper pretreatment process can improve the cost efficiency and the overall process [22].

Autohydrolysis provides an attractive alternative utilization for the chemical methods due to its advantages, including: (1) environment-friendly with no chemical requirement; (2) less corrosive for the equipment than the acid pre-hydrolysis; (3) greater yields of products with low byproducts compared to chemical methods since steam does not remove the uronic acid group and acetic [23], and (4) higher cost-efficient than other methods [21,24]. Autohydrolysis, also referred to as "steam explosion" is a process that uses an operation with steam at about 200 °C then suddenly drops to atmospheric pressure [21,25−27]. Steam can be performed as a weak acid with the biomass, and the acetyl group released from the hemicelluloses can also act as a source of acid. Sugar can then be released into the liquid phase due to the cracking of the glycosidic bond within the xylan and depolymerization of the hemicelluloses by hydronium ion catalysis [28,29].

By steam autohydrolysis with the proper treatment conditions, the sugar compound as xylooligosaccharides could be extracted from different bamboo products [21,26,28,29]. Similarly, bamboo culm is produced for sugar extraction at different temperatures and times. It was indicated that the maximum yield of 47.49% was achieved at 180 °C for the xylooligosaccharides with fewer other products [26]. The total reducing sugar was obtained from the bamboo by high-pressure hydrolysis treatment in a range of temperatures. The study revealed that the total sugar yield gained at about 42% with a temperature of 180 °C [21]. However, from our best search of the literature, the solid bamboo residue from the autohydrolysis process has still not been utilized.

Khuong et al. [30] described the effect of temperature on the sugar production from bamboo. From their result, the authors stated that the maximum yield of sugar could be extracted at around 200 °C. Additionally, a mixture of bamboo and water was treated by a hydrothermal method that is similar to autohydrolysis at 200 °C for 2.5 h. Afterward, the solid residue from the hydrothermal process was activated by physical and chemical methods for CO_2 capture with a relatively high capacities [31−33]. CO_2 capture by biochar is a promising strategy to reduce the CO_2 emissions in the environment. Although CO_2 adsorption from biochar has been developed, more efforts are needed to make more effective and economical products such as activated carbon with physical and chemical methods [34]. Conventionally, the activated carbon by chemical methods consumes less energy and activation time than those by physical processes, making chemical activation more efficient than physical modification [35]. KOH is a popular chemical reagent that has been commonly used for biochar activation. However, it has a limitation due to its corrosive character and is highly toxic [36]. Thus, the application of more environment-friendly chemical activators, such as K_2CO_3 [33] and potassium oxalate ($K_2C_2O_4$) [37,38], are more attractive to the user's attention. Furthermore, compared to KOH and K_2CO_3, several biomass materials activated by $K_2C_2O_4$ demonstrated that they are more favorable for CO_2 capture. The activation with $K_2C_2O_4$ produces high texture characteristics, such as a specific surface area and well-developed micropores, that are suitable for CO_2 capture [37,39,40]. Thus, we hypothesized that the activation by $K_2C_2O_4$ with a solid residue from bamboo steam treatment would produce a high-performance porous carbon for CO_2 adsorption due to its pore distribution and surface area properties. In this study, we aimed to extract sugar from bamboo chips then the solid residue was synthesized using $K_2C_2O_4$ at different ratios. Thereby, we investigated the activation mechanisms and simultaneously estimated the CO_2 adsorption capacities of the products using scanning electron microscopy (SEM), Fourier-transform infrared reflection (FTIR), and Raman spectroscopy.

2 Experimental

2.1 Raw material and chemical reagent

Bamboo chips were bought from a local provider in Fukuoka, Japan (Bamboo Techno Co., Ltd.). The chips were sieved using a screen with the size of 250 μm (60 mesh), then dried to a constant moisture content and stored in a desiccator. The chemical reagent, potassium oxalate monohydrate ($K_2C_2O_4 \cdot H_2O$, 99%), was purchased from the Wako Pure Chemical Corporation.

2.2 Autohydrolysis treatment

Five grams of sieved bamboo chips was put in a beaker and placed in a Teflon container that contained 10 mL of distilled water. The bamboo powder was separated from the distilled water in the Teflon container (Fig. S1, cf. Electronic Supplementary Material, ESM). The Teflon container was positioned inside an autoclave (HU-100, Sanai Science Co., Ltd., China). And then, the autoclave was heated in an oven kiln (Natural Convection Oven, DOV-300) which had already reached the desired temperature. The treatment temperature and time were at 200 °C and 2.5 h, respectively. After the heating process finished, the autoclave was immediately immersed in a

water bath to halt the reaction. The sample was removed from the autoclave when the temperature decreased to ambient temperature. Subsequently, the steam-treated sample was mixed with 45 mL of distilled water and stirred for 1 h at room temperature. Later, the mixture was separated into a solid residue and sugar solution by vacuum filtration through filter paper. The pH and brix values of the sugar solution were measured by a pH meter (Horiba, Japan) and brix meter (As One), respectively. The solid part was then dried overnight in an oven at 105 °C and stored for further activation use.

2.3 Activation of the solid residue

After the autohydrolysis treatment process, the solid residue was activated. The steam-treated bamboo from the previous autohydrolysis process was milled and sieved using 60 mesh sieves to achieve a homogeneous fine powder. $K_2C_2O_4$ was also ground into a fine powder, then thoroughly mixed with the solid residue at the mass $K_2C_2O_4$/solid residue ratios of 1, 2, 3, 4, 5, and 6. Afterward, the mixture was put into a ceramic boat, then placed in a tube furnace heated to 800 °C at the heating rate of 10 °C·min^{-1} under 0.5 L·min^{-1} flowing N_2 (Fig. 1). The activation process was held at the target temperature for 1 h under 0.5 L·min^{-1} flowing N_2. After activation, the resulting carbon was cooled in flowing N_2 until it reached room temperature. It was thoroughly washed using deionized water to completely remove any inorganic impurities. Finally, the activated carbon was filtered by vacuum filtration, and the remainder was dried overnight at 105 °C. The samples were labeled using the weight ratio of the $K_2C_2O_4$/solid residue and materials as follows: BS_K_*x* or BB_K_*x*, where BS refers to the bamboo residue after the autohydrolysis treatment, while BB refers to the raw bamboo material and *x* refers to the $K_2C_2O_4$/solid residue ratio.

The $K_2C_2O_4$/solid residue mass ratio of 1:1 (weight/weight) was selected for analyzing the effect of the activation temperature. Subsequently, the mixture was heated for an hour at the activation temperatures of 500, 600, 700, 800, and 900 °C and heating rate of 10 °C·min^{-1}. This process is prepared under flowing N_2 at the rate of 0.5 L·min^{-1}. The results were indexed as BS_K1_*y*, with *y* presenting the activation temperature. Based on the N_2 sorption and CO_2 capture capacity of samples BS_K1_*y*, the activation temperature of 800 °C was indicated as the optimal for the next experiment with a different $K_2C_2O_4$/solid residue ratio. The detailed textural and sorption properties can be found in the supplementary materials (Figs. S2 and S3, and Table S1, cf. ESM).

The samples and bamboo materials were measured for their ash content by combustion in a tube furnace for 3 h at 600 °C in the ambient atmosphere. After burning, the remaining residue ingredient was ash, and its content was calculated as follows:

$$\text{Ash content} = \frac{\text{Weight of residue remaining}}{\text{Weight of initial materials}} \times 100\%. \quad (1)$$

For comparison, the raw bamboo material was pyrolyzed at 800 °C, then evaluated as only the ash content (labeled BB_800).

2.4 N_2 adsorption/desorption and CO_2 uptake measurements

Before all the adsorption/desorption measurements, the samples were pretreated under vacuum conditions for outgassing at 300 °C for 3 h. The adsorption/desorption isotherms using N_2 were determined at 77 K (–196 °C) by the Belsorp-mini II analyzer device (MicrotracBEL, Japan). The surface area was calculated by the BET method (Brunauer-Emmett-Teller) from the N_2 adsorption isotherms according to ISO 9277. The total pore volume was calculated from the total nitrogen uptake at the relative pressure of P/P_0 ~1. Additionally, the t-plot analysis was applied to determine the micropore volume and micropore surface area. The MP plot method, which expanded the t-plot method, was used to calculate the pore size distribution using the nitrogen adsorption data. Likewise, the CO_2 uptake capacity at 298 K (25 °C) and

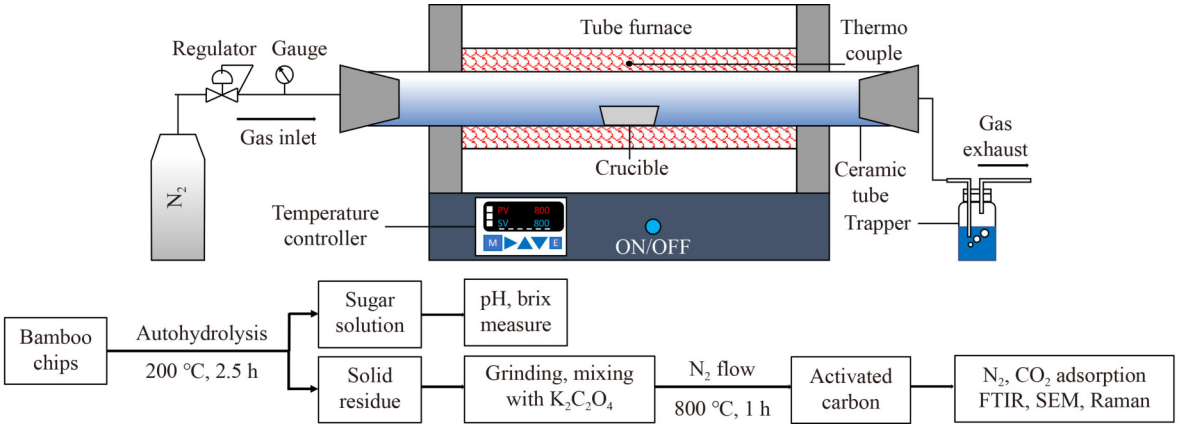

Fig. 1 Schematic of tube furnace for activation and experiment process diagram.

pressure of 1.013×10^5 Pa was measured using the previously described sorption instrument.

2.5 FTIR, SEM, and Raman spectroscopy, and elemental analysis

The functional groups on the sample's surfaces were analyzed by FTIR (JASCO Corporation, FTIR-4600 ATR method, Ge prism) and the spectra band in the range of 4000–500 cm^{-1} was investigated. The images of the activated carbon were recorded using an energy dispersive X-ray analyzer (SEM-EDX, Japan) ERA-8800FE (ELIONIX Inc., Tokyo, Japan) operating at a 15 kV accelerating voltage.

The structure and graphitization of the samples were analyzed using a Raman spectroscopy device (NRS-5100, JASCO Corporation, Japan) with the beam excitation wavelength of 532 nm. An elemental analyzer (Perkin-Elmer 2400 Series II) was used to measure the elemental composition of the samples.

3 Results and discussion

3.1 Characterization of the activated carbon

3.1.1 Yields and ash contents

After the autohydrolysis treatment, the sugar solutions pH and brix were measured. The average value of the solution pH was 3.14, and the mean value of the sugar solution Brix was 2.03. Following the activation process, the yields were calculated. Generally, the yield of the activated carbon is described by the weight of the final dry product after the activation process, soaking and washing, then divided by the dry mass of the initial raw resources [41]. In this report, the yields of the activated carbon before and after the washing process by distilled water were estimated to describe the activity of $K_2C_2O_4$. It can be found from Fig. 2 that the activated carbon yields before the washing procedure were very high due to the existence of a large amount of inorganic residuals. As seen in Fig. 2, the range of the yields before the washing increased from about 45% to nearly 67%. This suggested that the decomposition of $K_2C_2O_4$ during the activation process had not significantly changed, followed by the increased $K_2C_2O_4$ weight. After removing the inorganic salts, the yields of the activated carbon drastically decreased. The presumed activation processes are described by the following equations:

$$K_2C_2O_4 \rightarrow K_2CO_3 + CO \quad (2)$$

$$K_2CO_3 + 2C \rightarrow 2K + 3CO \quad (3)$$

$$K_2CO_3 \rightarrow K_2O + CO_2 \quad (4)$$

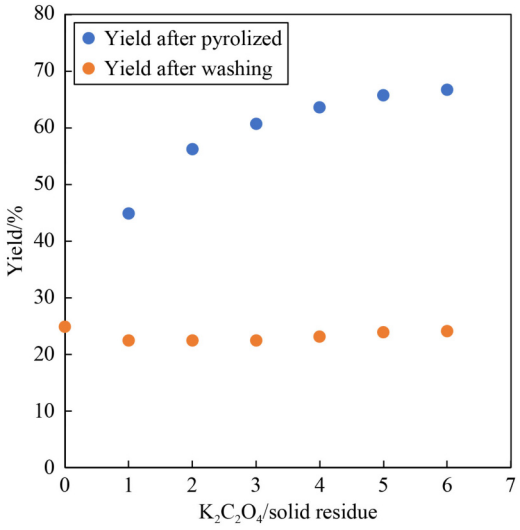

Fig. 2 Yields of carbons material after pyrolized and after washing process.

$$C + CO_2 \rightarrow 2CO \quad (5)$$

Based on the equations, the carbon content in the material reacted to generate the CO gas, which could be a reason for the drastic yield decrease. The released gas could be the agent to create abundant pores in the char's surface.

After the washing process acquired from the bamboo residue, the activated carbon yields were similar, in the range of 22.42%–24.13%. Compared to the activated carbon prepared with $K_2C_2O_4$, the yields of the activated carbon without $K_2C_2O_4$ were slightly higher with a value of 24.85%. It is noteworthy that the yield of the activated carbon obtained from the raw bamboo material using $K_2C_2O_4$ as an activator was the lowest at 10.11%. The reason for this result could be explained by the fixed carbon content in the materials before activation. Typically, the high fixed carbon leads to a high yield of the final activated products [42]. Additionally, this result suggested that the hydrolysis process could produce a higher fixed carbon than the no-pretreatment process. The yields in this study were similar to the activated carbon from sawdust [3] and lower than that from the glucose and hydro char [2,43]. As expected, the reactivity during the decomposition process of $K_2C_2O_4$ was milder than that of KOH, leading to a higher yield of biochar [2,3].

It is important to note that the ratio between $K_2C_2O_4$ and the precursor was not a critical factor in deciding the activated carbon yield. The results in Table 1 show that the ratio from 1 to 6 did not considerably affect the yields. This result is consistent with a previous study [3]. However, this tendency was not observed for the KOH activation, in which the ratio was the critical factor for the char yields [44,45].

As described in section 2.3, the ash contents in the activated carbon were calculated to determine the purity of the final products by a combustion process. The high

Table 1 Textural properties, elemental composition and CO_2 uptake capacities at 25 °C, 1.013×10^5 of carbons derived from bamboo

Sample	Yield/%	Ash[a)]/%	S_{BET}[b)]/ ($m^2 \cdot g^{-1}$)	V_{total}[c)]/ ($cm^3 \cdot g^{-1}$)	S_{micro}[d)]/ ($m^2 \cdot g^{-1}$)	V_{micro}[e)]/ ($cm^3 \cdot g^{-1}$)	C/ (wt %)	H/ (wt %)	N/ (wt %)	Other[f)]/ (wt %)	CO_2 uptake/ ($mmol \cdot g^{-1}$)
BS_K_0	24.85	1.27 (5.57)	502.4	0.21	546.4	0.21	82.82	1.36	0.47	15.35	2.5
BS_K_1	22.42	0.50	1262.0	0.58	1403.5	0.54	87.08	0.28	1.16	11.48	3.9
BS_K_2	22.45	0.50	1361.8	0.65	1510.8	0.57	86.96	0.21	1.10	11.73	4.1
BS_K_3	22.49	0.48	1416.6	0.71	1547.4	0.59	85.04	0.43	2.43	12.10	4.0
BS_K_4	23.15	0.45	1374.2	0.75	1511.4	0.57	85.12	0.36	2.13	12.39	4.0
BS_K_5	23.90	0.15	1326.1	0.75	1454.6	0.55	85.32	0.05	1.67	12.96	4.0
BS_K_6	24.13	0.14	1431.7	0.88	1538.9	0.58	86.50	0.03	1.34	12.13	4.1
BB_K_3	10.11	0.74	1412.7	0.89	1493.7	0.63	86.41	0.31	0.99	12.29	3.5

a) Value in parentheses is ash content of biochar from bamboo at 800 °C; b) BET specific surface area; c) total pore volume; d) micropore surface area; e) micropore volume; f) Other = 100 – C(wt %) – H(wt %) – N(wt %)

ash contents in the activated carbon could lead to a low quality of the samples due to the pores being clogged and reducing the pore volume and specific surface area. Likewise, the high ash contents could hinder pore development and reduce the sorption capacities [46]. In this study, the samples were almost free of inorganic impurities with an ash content in the range of 0.14%–1.27% and the highest value for the biochar from the solid residue without activation (BS_K_0). The ash content of the BB_800 was found to be higher than that of the bamboo residue precursor after the autohydrolysis treatment process (BS_K_0). This result indicated that the extractive contents decreased as a result of the autohydrolysis. As a result, the ash content significantly decreased from 5.57% in the biochar derived from the pristine bamboo material (BB_800) to 1.27% in the solid residue (BS_K_0). Furthermore, the ash contents and inorganic compounds present in the final product were determined by both the chemical reaction between the precursor and chemical activator, together with the carbon pyrolysis process.

3.1.2 Elemental analysis

Table 1 shows the elemental contents data for some samples prepared in this study. It can be seen that all the activated carbon samples with $K_2C_2O_4$ contained a higher amount of carbon elements than that of the sample without activation. The data also indicated that the content of the nitrogen element in the activated carbon samples increased compared to the biochar sample (BS_K_0). On the other hand, it is noted that the $K_2C_2O_4$ ratio did not have a noticeable effect on the elemental contents of the activated carbon. Besides, the elemental contents of the samples from the raw bamboo material and solid residue that activated with $K_2C_2O_4$ are similar.

3.1.3 N_2 sorptions isotherm and textural properties

Fig. 3 presents the N_2 sorption isotherms measured on biochar and activated carbon obtained by the $K_2C_2O_4$ synthesis with different precursor carbon materials. As can be seen from Fig. 3, the isotherm was typically type I

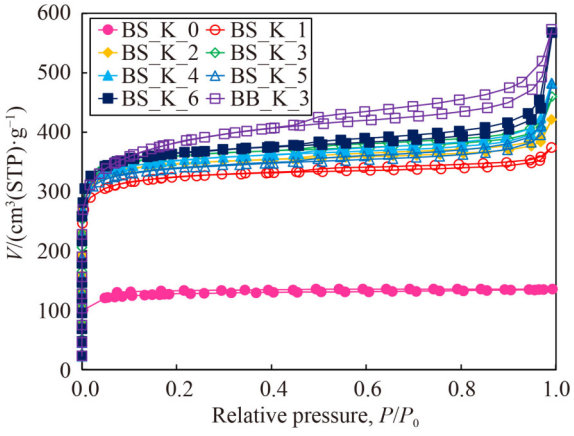

Fig. 3 N_2 sorption isotherm at 77 K of products from bamboo and solid residue.

according to the IUPAC classification [47]. Type I describes the microporous structure where almost all the N_2 uptake occurred at a very low relative pressure, at $P/P_0 < 0.1$, owing to the micropore filling process. The isotherm of raw bamboo material (BB_K_3) had a slight broadening than the others with the adsorption linearly increased up to a relative pressure of 0.4. It suggested the presence of much wider micropores or mesopores inside the BB_K_3 sample [48,49]. Besides, the isotherms of the solid residue activated with different ratios of $K_2C_2O_4$ were very similar in shape and the N_2 sorption capacity resembled the type I sorption. Regarding the isotherm of the BS_K_0 biochar, the sorption isotherm was the lowest N_2 uptake among the samples. It is essential to note that an increase in the amount of $K_2C_2O_4$ did not critically affect the porosity. It is consistent with previous studies [2,3] and suggests that the change in porosity and sorption uptake could be from the autohydrolysis treatment.

Table 1 lists the textural properties of the activated carbons and biochar. It showed that the raw solid residue biochar (BS_K_0) exhibited a BET specific surface area of 502 $m^2 \cdot g^{-1}$ and a pore volume of 0.21 $cm^3 \cdot g^{-1}$. After the activation by $K_2C_2O_4$, the BET surface area significantly increased. The surface area of the solid residue activated carbons was in the range of 1262–

1432 $m^2 \cdot g^{-1}$ with the total pore volume between 0.58 and 0.88 $cm^3 \cdot g^{-1}$. The surface area and pore volume slightly increased as the amount of $K_2C_2O_4$ rose. However, the tendency was not clear for the ratio at 4 and 5. Hence, the BET specific surface area and pore volume of BS_K_6 (1432 $m^2 \cdot g^{-1}$ and 0.88 $cm^3 \cdot g^{-1}$, respectively) were greater than those of BS_K_1 (1262 $m^2 \cdot g^{-1}$ and 0.58 $cm^3 \cdot g^{-1}$, respectively). The pore size distribution curves of the activate carbons activated with different amounts of $K_2C_2O_4$ at 800 °C are indicated in Fig. 4, and the micropore properties are described in Table 1. At a glance, all the samples had a peak at 0.7 nm. However, the pores with a diameter less than 0.7 nm cannot be detected by the MP method, which is based on the t-plot theory. Therefore, it can be said that the samples contain many micropores with diameters smaller than 0.7 nm. The higher amount of $K_2C_2O_4$ appears to raise the microporosity both in the micropore volume and micropore surface area.

The comparison between the different ratios of the $K_2C_2O_4$/raw bamboo material regarding the activated carbon textural properties and CO_2 uptake capacity are presented in Figs. S4 and S5, and Table S2 (cf. ESM). It is noteworthy that the BB_K_3 sample had the highest porosity properties and CO_2 capture capacity among the activated carbons from bamboo. Thus, the BB_K_3 sample was selected to compare the textural properties and CO_2 sorption capacity with the other products from the solid residue. The BB_K_3 sample had a greater micropore volume than that of BS_K_3 but a lower micropore surface area than that of BS_K_3. In general, the direct activation between bamboo or the synthesis of the solid residue with $K_2C_2O_4$ did not affect the porosity of the products. It is also important to note that a moderately small amount of $K_2C_2O_4$ can be used in the activation process to improve the porosity.

3.1.4 Raman spectral and FTIR analysis

The disordered structures of the biochar and activated carbons with different ratios of $K_2C_2O_4$/bamboo are illustrated by the Raman spectrum in Fig. 5. The band at around 1589 cm^{-1} was assigned the G band, which was ascribed to the stretching band of sp^2 atoms in the rings and chains of graphitic materials. The G band referred to the graphite structure. Besides, the D band at around 1331 cm^{-1} referred to the disordered structure of the carbon materials. Thus, the intensity ratios between the D and G bands (I_D/I_G) were used to measure the ordering in the carbon materials structure. The higher value of the ratio I_D/I_G means that a higher disorder degree of the carbon structures was observed [43,46]. Figure 5 revealed that all the samples had amorphous structures since the ratio I_D/I_G was greater than 1. Furthermore, Fig. 5 also showed the independence between the I_D/I_G ratio and $K_2C_2O_4$/solid residue ratio. The highest value was observed at the $K_2C_2O_4$/bamboo ratio of 6 and the lowest on the solid residue biochar without activation (BS_K_0). The FTIR spectra were also investigated for all the samples as presented in Fig. S6 (cf. ESM).

3.1.5 SEM images analysis

To further investigate, SEM images were used to evaluate the changes in the bamboo and solid residue morphology using the autohydrolysis process followed by carbonization and activation. The SEM images of the samples are shown in Fig. 6. As can be seen from the figure, the BS_K_0 sample showed a sheet-like non-porous structure, while the sample with the $K_2C_2O_4$ activation exhibited a sponge-like porous carbon structure. This finding suggested that $K_2C_2O_4$ was a promising chemical activation favored for generating the porous structure [36,37]. Remarkably, the sample with

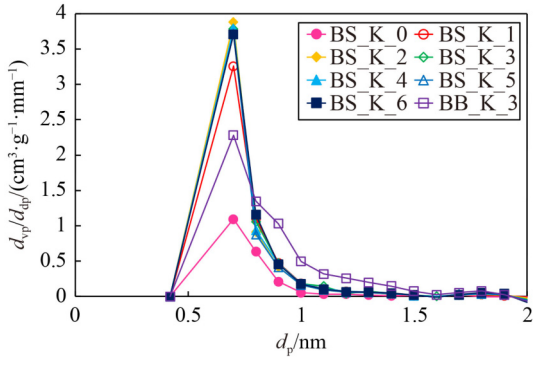

Fig. 4 Pore distribution of resulting carbons from MP-plot method.

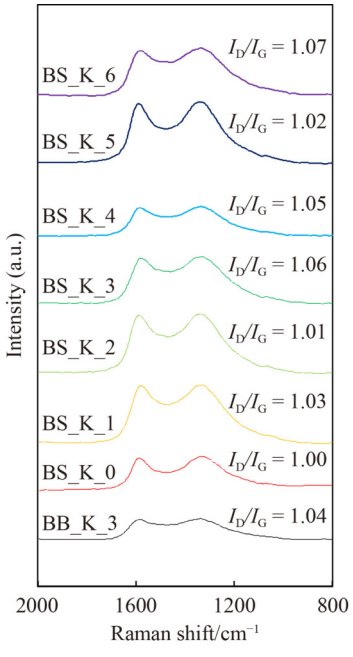

Fig. 5 Raman spectrum of activated carbons and biochar from bamboo and solid residue.

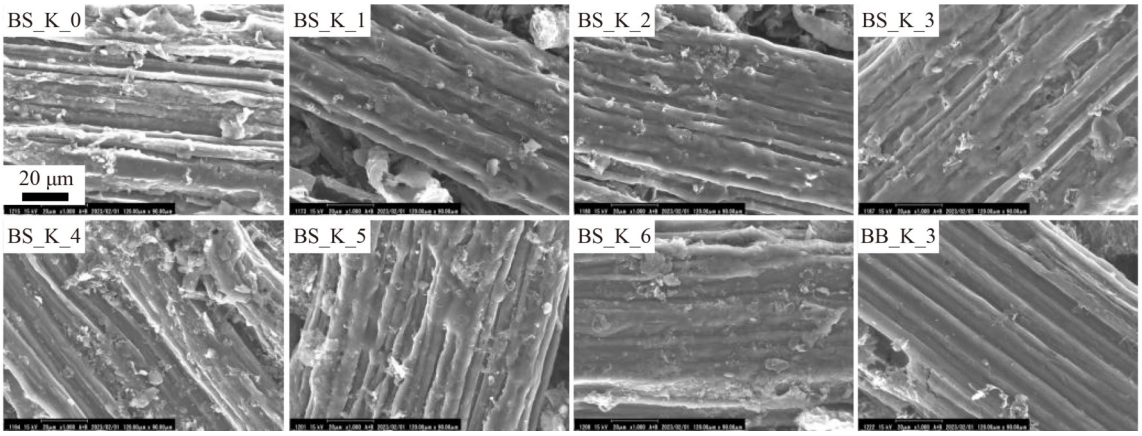

Fig. 6 SEM images of biochar and activated carbons derived from bamboo.

the autohydrolysis treatment exhibited a sponge-like structure that was a favorable pretreatment process for porous carbon activation [37].

3.2 CO_2 uptake capacity

The CO_2 uptake of all the samples was measured at 25 °C and 1.013 × 10^5 Pa pressure. The CO_2 sorption isotherms are illustrated in Fig. 7, and the uptake capacity is presented in Table 1. In fossil energy power plants, the CO_2 uptake under ambient conditions with a pressure of 1.013 × 10^5 Pa is regularly used for measuring the performance of post-combustion adsorption from a gas streams chimney [50]. In this study, the CO_2 uptake was in the range of 2.5–4.1 mmol·g^{-1}, with the highest CO_2 uptake for samples BS_K_2 and BS_K_6. It proved that the CO_2 uptake significantly improved from 2.5 mmol·g^{-1} for the biochar without activation (BS_K_0) to 4.1 mmol·g^{-1} for the sample activated with the $K_2C_2O_4$/solid residue ratio of 2, then declined for the samples with the ratio of 3, 4, and 5. However, the CO_2 uptake for the BS_K_6 sample with the $K_2C_2O_4$/solid ratio of 6 also ranked with the highest capture capacity among all the samples. This finding described that the rising ratio of the $K_2C_2O_4$/solid residue was not beneficial for the CO_2 capture capacity [2,3]. The value of 4.1 mmol·g^{-1} is a very competitive CO_2 uptake capacity compared to other research reported at the ambient condition at 1.013 × 10^5 Pa and 25 °C. The comparison data are shown in Table S8 (cf. ESM). It was also found that the CO_2 uptake was improved by the autohydrolysis treatment, where the capture capacity of the BS_K_3 sample was 4.0 mmol·g^{-1} compared to 3.5 mmol·g^{-1} for the BB_K_3 sample. The data suggested that the total pore and micropore volumes did not significantly affect the CO_2 uptake capacity. Besides, the data proved that the micropore surface area determined the CO_2 capture performance. This result is obviously seen in the data of the activated carbon from bamboo (Figs. S2 and S3). In these figures, the surface area of sample BB_K1_900 of 1458 m^2·g^{-1} is much greater than

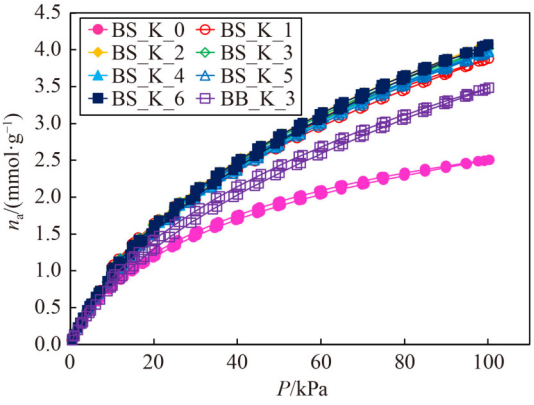

Fig. 7 CO_2 sorption isotherm of products at 25 °C and 1.013 × 10^5 Pa.

that of sample BB_K1_600 of 724 m^2·g^{-1}, but the CO_2 capture capacity of sample BB_K1_900 is 2.6 mmol·g^{-1} and significantly lower than that of sample BB_K1_600 of 3.3 mmol·g^{-1}. Also, this result is consistent with the previous studies that reported that the CO_2 uptake was determined by the ultra-micropores [43] that are less than 0.7 nm [37,40] or between 0.6 and 0.8 nm [2,3].

The cost for 1 g activated carbon from steam-treated bamboo solid residue with $K_2C_2O_4$ was estimated on an experimental scale then compared to that of other activated carbons from conventional activation agents such as K_2CO_3 and KOH. It is noted that the cost for 1 g of products from the solid residue activated with $K_2C_2O_4$ in this study is much cheaper than that of products from KOH and K_2CO_3 when comparing at a similar CO_2 capture capacity (Table S7, cf. ESM). The reason can be explained by the relatively high CO_2 capture capacity and yield of $K_2C_2O_4$ with the solid residue at a low ratio of chemical agent per material.

4 Conclusions

In summary, a highly microporous structure of activated

carbon was produced from bamboo and solid residue after the autohydrolysis treatment process by a more eco-friendly chemical activator than using peroxide activator agents. Activation of the solid residue with potassium oxalate produced a high specific surface area (1262–1432 $m^2 \cdot g^{-1}$) with an outstanding CO_2 uptake capacity (4.1 $mmol \cdot g^{-1}$) at the ambient conditions of 25 °C and 1.013×10^5 Pa. The $K_2C_2O_4$/solid residue ratio was not the critical factor in determining the CO_2 uptake performance. The pore volume and specific surface area of the activated carbon without the autohydrolysis treatment were higher than those of samples with treatment. However, the micropore surface area was lower than that of the samples from the solid residue. Furthermore, autohydrolysis is essential for the pretreatment process and is the key to enhancing the CO_2 capture capacity compared to the activation without pretreatment. This scenario enables autohydrolysis as an easy preprocess that is beneficial both in oligosaccharide extraction and biochar porosity control. It offers a more sustainable and environment-friendly activation reagent [2].

Competing interests The authors declare that they have no competing interests.

Electronic Supplementary Material Supplementary material is available in the online version of this article at http://doi.org/10.1007/s11705-024-2402-8 and is accessible for authorized users.

References

1. Stocker T F, Qin D, Plattner G-K, Tignor M M B, Allen S K, Boschung J, Nauels A, Xia Y, Bex V, Midgley P M. IPCC, 2013: Climate change 2013: the physical science basis. Contribution of working group I to the fifth assessment report of the Intergovernmental Panel on Climate Change. 2013
2. Aljumialy A M, Mokaya R. Porous carbons from sustainable sources and mild activation for targeted high-performance CO_2 capture and storage. Materials Advances, 2020, 1(9): 3267–3280
3. Altwala A, Mokaya R. Direct and mild non-hydroxide activation of biomass to carbons with enhanced CO_2 storage capacity. Energy Advances, 2022, 1(4): 216–224
4. Rochelle G T. Amine scrubbing for CO_2 capture. Science, 2009, 325(5948): 1652–1654
5. Siegelman R L, Kim E J, Long J R. Porous materials for carbon dioxide separations. Nature Materials, 2021, 20(8): 1060–1072
6. Raganati F, Miccio F, Ammendola P. Adsorption of carbon dioxide for post-combustion capture: a review. Energy & Fuels, 2021, 35(16): 12845–12868
7. Cha J S, Park S H, Jung S C, Ryu C, Jeon J K, Shin M C, Park Y K. Production and utilization of biochar: a review. Journal of Industrial and Engineering Chemistry, 2016, 40: 1–15
8. Ghodake G S, Shinde S K, Kadam A A, Saratale R G, Saratale G D, Kumar M, Palem R R, AL-Shwaiman H A, Elgorban A M, Syed A, et al. Review on biomass feedstocks, pyrolysis mechanism and physicochemical properties of biochar: state-of-the-art framework to speed up vision of circular bioeconomy. Journal of Cleaner Production, 2021, 297: 126645
9. Yaashikaa P R, Kumar P S, Varjani S, Saravanan A. A critical review on the biochar production techniques, characterization, stability and applications for circular bioeconomy. Biotechnology Reports, 2020, 28: e00570
10. Bamdad H, Hawboldt K. Comparative study between physicochemical characterization of biochar and metal organic frameworks (MOFs) as gas adsorbents. Canadian Journal of Chemical Engineering, 2016, 94(11): 2114–2120
11. Andirova D, Cogswell C F, Lei Y, Choi S. Effect of the structural constituents of metal organic frameworks on carbon dioxide capture. Microporous and Mesoporous Materials, 2016, 219: 276–305
12. Lobovikov M, Paudel S, Piazza M, Ren H, Wu J. World bamboo resources: a thematic study prepared in the framework of the global forest resources, assessment 2005. 2007
13. Mayowa Akeem Azeez. Orege J I. Bamboo, its chemical modification and products. In: Bamboo—Current and Future Prospects. London: InTech Open, 2020
14. Fatriasari W, Solihat N N, Sari F P, Karimah A, Sohail A. Sugar production from bamboo. Springer Nature Singapore, 2023
15. Viet D D, Tsubota T, Shinogi Y. Humidity adsorption characteristics of Moso bamboo charcoal oxidized at room temperature by HNO. Journal of the Indian Academy of Wood Science, 2020, 17(1): 34–41
16. INBAR. Trade Overview 2019: Bamboo and Rattan Commodities in The International Market, 2021
17. Felisberto M H F, Beraldo A L, Clerici M T P S. Young bamboo culm flour of Dendrocalamus asper: technological properties for food applications. Lebensmittel-Wissenschaft + Technologie, 2017, 76: 230–235
18. Dong Y, Takeshita T, Miyafuji H, Nokami T, Itoh T. Direct extraction of polysaccharides from Moso bamboo (*Phylostachys herocycla*) chips using a mixed solvent system of an amino acid ionic liquid with polar aprotic solvent. Bulletin of the Chemical Society of Japan, 2018, 91(3): 398–404
19. Zhang X, Li M, Zhong L, Peng X, Sun R. Microwave-assisted extraction of polysaccharides from bamboo (*Phyllostachys acuta*) leaves and their antioxidant activity. BioResources, 2016, 11(2): 5100–5112
20. Palaniappan A, Antony U, Emmambux M N. Current status of xylooligosaccharides: production, characterization, health benefits and food application. Trends in Food Science & Technology, 2021, 111: 506–519

21. Mohan M, Banerjee T, Goud V V. Hydrolysis of bamboo biomass by subcritical water treatment. Bioresource Technology, 2015, 191: 244–252
22. Bhutto A W, Qureshi K, Harijan K, Abro R, Abbas T, Bazmi A A, Karim S, Yu G. Insight into progress in pre-treatment of lignocellulosic biomass. Energy, 2017, 122: 724–745
23. Nabarlatz D, Farriol X, Montané D. Autohydrolysis of almond shells for the production of xylo-oligosaccharides: product characteristics and reaction kinetics. Industrial & Engineering Chemistry Research, 2005, 44(20): 7746–7755
24. Kilpeläinen P. Pressurized hot water flow-through extraction of birch wood. Dissertation for the Doctoral degree. Findland: Abo Akademi University, 2015
25. García-Aparicio M, Parawira W, Van Rensburg E, Diedericks D, Galbe M, Rosslander C, Zacchi G, Görgens J. Evaluation of steam-treated giant bamboo for production of fermentable sugars. Biotechnology Progress, 2011, 27(3): 641–649
26. Xiao X, Bian J, Peng X P, Xu H, Xiao B, Sun R C. Autohydrolysis of bamboo (*Dendrocalamus giganteus* Munro) culm for the production of xylo-oligosaccharides. Bioresource Technology, 2013, 138: 63–70
27. Singh R D, Nadar C G, Muir J, Arora A. Green and clean process to obtain low degree of polymerisation xylooligosaccharides from almond shell. Journal of Cleaner Production, 2019, 241: 118237
28. Chen M H, Bowman M J, Dien B S, Rausch K D, Tumbleson M E, Singh V. Autohydrolysis of Miscanthus × *giganteus* for the production of xylooligosaccharides (XOS): kinetics, characterization and recovery. Bioresource Technology, 2014, 155: 359–365
29. Garrote G, Domínguez H, Parajó J C. Autohydrolysis of corncob: study of non-isothermal operation for xylooligosaccharide production. Journal of Food Engineering, 2002, 52(3): 211–218
30. Khuong D A, Saza S, Tsubota T. The production of high-value products derived from bamboo by steam pretreatment: sugar-contained water solution and solid residue as a precursor for EDLC electrode. Materials Chemistry and Physics, 2023, 304: 127853
31. Khuong D A, Nguyen H N, Tsubota T. Activated carbon produced from bamboo and solid residue by CO_2 activation utilized as CO_2 adsorbents. Biomass and Bioenergy, 2021, 148: 106039
32. Khuong D A, Nguyen H N, Tsubota T. CO_2 activation of bamboo residue after hydrothermal treatment and performance as an EDLC electrode. RSC Advances, 2021, 11(16): 9682–9692
33. Khuong D A, Trinh K T, Nakaoka Y, Tsubota T, Tashima D, Nguyen H N, Tanaka D. The investigation of activated carbon by K_2CO_3 activation: micropores- and macropores-dominated structure. Chemosphere, 2022, 299: 134365
34. Guo S, Li Y, Wang Y, Wang L, Sun Y, Liu L. Recent advances in biochar-based adsorbents for CO_2 capture. Carbon Capture Science and Technology, 2022, 4: 100059
35. Fu Y, Shen Y, Zhang Z, Ge X, Chen M. Activated bio-chars derived from rice husk via one- and two-step KOH-catalyzed pyrolysis for phenol adsorption. Science of the Total Environment, 2019, 646: 1567–1577
36. Sevilla M, Díez N, Fuertes A B. More sustainable chemical activation strategies for the production of porous carbons. ChemSusChem, 2021, 14(1): 94–117
37. Rehman A, Nazir G, Rhee K Y, Park S J. Valorization of orange peel waste to tunable heteroatom-doped hydrochar-derived microporous carbons for selective CO_2 adsorption and separation. Science of the Total Environment, 2022, 849: 157805
38. Jiang Q, Wang Y, Gao Y, Zhang Y. Fabrication and characterization of a hierarchical porous carbon from corn straw-derived hydrochar for atrazine removal: efficiency and interface mechanisms. Environmental Science and Pollution Research International, 2019, 26(29): 30268–30278
39. Guerrera J V, Burrow J N, Eichler J E, Rahman M Z, Namireddy M V, Friedman K A, Coffman S S, Calabro D C, Mullins C B, Mullins C B. Evaluation of two potassium-based activation agents for the production of oxygen- and nitrogen-doped porous carbons. Energy & Fuels, 2020, 34(5): 6101–6112
40. Nazir G, Rehman A, Park S J. Role of heteroatoms (nitrogen and sulfur)-dual doped corn-starch based porous carbons for selective CO_2 adsorption and separation. Journal of CO_2 Utilization, 2021, 51: 101641
41. Diao Y, Walawender W P, Fan L T. Activated carbons prepared from phosphoric acid activation of grain sorghum. Bioresource Technology, 2002, 81(1): 45–52
42. Feng P, Li J, Wang H, Xu Z. Biomass-based activated carbon and activators: preparation of activated carbon from corncob by chemical activation with biomass pyrolysis liquids. ACS Omega, 2020, 5(37): 24064–24072
43. Sevilla M, Al-Jumialy A S M, Fuertes A B, Mokaya R. Optimization of the pore structure of biomass-based carbons in relation to their use for CO_2 capture under low- and high-pressure regimes. ACS Applied Materials & Interfaces, 2018, 10(2): 1623–1633
44. Balahmar N, Mitchell A C, Mokaya R. Generalized mechanochemical synthesis of biomass-derived sustainable carbons for high performance CO_2 storage. Advanced Energy Materials, 2015, 5(22): 1–9
45. Adeniran B, Mokaya R. Compactivation: a mechanochemical approach to carbons with superior porosity and exceptional performance for hydrogen and CO_2 storage. Nano Energy, 2015, 16: 173–185
46. Serafin J, Baca M, Biegun M, Mijowska E, Kaleńczuk R J, Sreńscek-Nazzal J, Michalkiewicz B. Direct conversion of biomass to nanoporous activated biocarbons for high CO_2 adsorption and supercapacitor applications. Applied Surface Science, 2019, 497: 143722
47. Thommes M, Kaneko K, Neimark A V, Olivier J P, Rodriguez-Reinoso F, Rouquerol J, Sing K S W. Physisorption of gases, with special reference to the evaluation of surface area and pore size distribution (IUPAC Technical Report). Pure and Applied Chemistry, 2015, 87(9-10): 1051–1069
48. Rodriguez-Mirasol J, Cordero T, Radovic L R, Rodriguez J J. Structural and textural properties of pyrolytic carbon formed within a microporous zeolite template. Chemistry of Materials, 1998, 10(2): 550–558
49. Su F, Zhao X S, Lv L, Zhou Z. Synthesis and characterization of microporous carbons templated by ammonium-form zeolite Y.

Carbon, 2004, 42(14): 2821–2831

50. Coromina H M, Walsh D A, Mokaya R. Biomass-derived activated carbon with simultaneously enhanced CO_2 uptake for both pre and post combustion capture applications. Journal of Materials Chemistry. A, Materials for Energy and Sustainability, 2016, 4(1): 280–289